Coplanar waveguides and superconducting resonators: For use in hybrid Rydberg-circuit QED experiments

Author: Alexandre Morgan †
Supervisor: Stephen Hogan †

† *Department of Physics and Astronomy, University College London, London WC1E 6BT, United Kingdom*
(Dated: February 16, 2017)

CONTENTS

I. LIGHT-MATTER INTERACTIONS

A typical system used for studying light-matter interactions is that of an atom in a cavity light field. This field of study is referred to as cavity quantum electrodynamics (cQED). Such a system in the resonant limit ($\omega_a - \omega_r \ll g$) can be described by the *Jaynes-Cummings Hamiltonian*,

$$H_{\mathrm{JC}} = \hbar\omega_r \left(a^\dagger a + \frac{1}{2}\right) + \hbar\frac{\omega_a}{2}\sigma_z + \hbar g(a^\dagger\sigma^- + a\sigma^+) \quad (1)$$

where $\hbar\omega_r$ is the photon energy, $a^\dagger$, a are the photon creation and annihilation operators (where photon number, $n = a^\dagger a$), $\hbar\omega_a$ is the qubit transition energy, σ_z is the Pauli-Z operator, g is the coupling rate and $a^\dagger\sigma^-$, $a\sigma^+$ represent the absorption and emission of a photon by the atom. The interaction term leads to a coherent transfer of excitations from the light field to the atom, called *Rabi oscillations*. This process is accompanied by incoherent decay processes as illustrated in Figure 1.

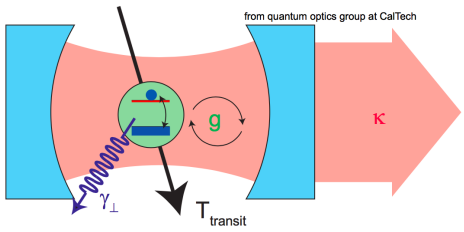

FIG. 1. Illustration of light-matter interactions between an atom and the light field confined to a cavity. In the strong coupling limit ($g > \kappa, \gamma_\perp, \frac{1}{T_{\mathrm{transit}}}$), excitation oscillate between the atom and the light field, a phenomena called *Rabi oscillations*. The rate of this coherent process is defined by g, the coupling rate. The incoherent decay processes are κ the radiative decay from the cavity, $\gamma_\perp$ the atomic decay into modes not trapped by the cavity, and $\frac{1}{T_{\mathrm{transit}}}$ the transit time of the atom through the cavity.

The quality factor of such a cavity is given by,

$$Q = \frac{\omega_r}{\kappa} \quad (2)$$

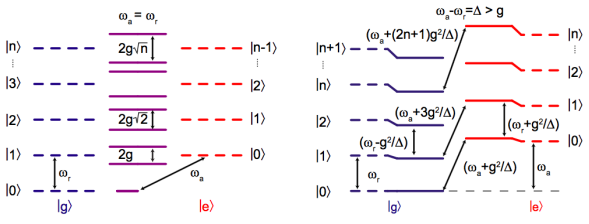

FIG. 2.

Dispersive limit

In the dispersive limit, $g \ll \Delta$ (where $\Delta = \omega_a - \omega_r$ is the detuning), the Jaynes-Cummings Hamiltonian can be rewritten either as,

$$H \approx \hbar \left(\omega_r + \frac{g^2}{\Delta}\sigma_z\right)\left(a^\dagger a + \frac{1}{2}\right) + \hbar\omega_a \frac{\sigma_z}{2} \tag{3}$$

which highlights its effect on the cavity field, i.e. to result in an atom state dependent effective resonant frequency, $\omega_r^* = \omega_r \pm \frac{g^2}{\Delta}$. It can also be written as,

$$H \approx \hbar\omega_r \left(a^\dagger a + \frac{1}{2}\right) + \hbar\left(\omega_a + \frac{2g^2}{\Delta}a^\dagger a + \frac{2g^2}{\Delta}\right)\frac{\sigma_z}{2} \tag{4}$$

highlighting the effect on the atom.

II. RYDBERG ATOMS

The wavelength of the transition between the n_1th and n_2th levels is given by,

$$\frac{1}{\lambda} = R_M\left(\frac{1}{n_1^2} - \frac{1}{n_1^2}\right) \tag{5}$$

where R_M is the reduced mass,

$$R_M = \frac{R_\infty}{1 + \frac{m_e}{M}} \tag{6}$$

where R_∞ is the Rydberg constant with an infinite mass nucleus, m_e is the electron mass, and M is the mass of the nucleus. R_∞ is given by,

$$R_\infty = \frac{m_e e^4}{8\epsilon_0^2 h^3 c} = 1.0973731568508 \times 10^7 m^{-1} \tag{7}$$

The frequency of the transition is then,

$$f = \frac{c}{\lambda} \tag{8}$$

where c is the speed of light.

III. COPLANAR WAVEGUIDES (CPW)

A coplanar waveguide (CPW) is a single plane transmission line consisting of a centre conductor of width W separated from two semi-infinite ground planes by two insulating gaps of widths s, as shown in Figure 3.

Conformal mapping technique

The properties of a CPW can be understood through the use of the so-called *conformal mapping technique* [1]. The results for a CPW on an infinitely thick dielectric substrate are as follows. The contribution to the capacitance due to the dielectric substrate is,

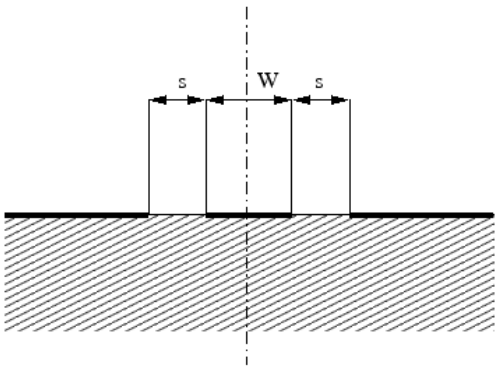

FIG. 3. Coplanar wave guide (CPW) geometry, with a centre conductor of width W and insulating gaps of widths s.

$$C_d = 2\epsilon_0(\epsilon_r - 1)\frac{K(k)}{K(k')} \tag{9}$$

where ϵ_0 is the permittivity of free space, ϵ_r is the relative permittivity of the dielectric, $K(...)$ is the complete elliptic integral of the first kind, and k, k' are given by,

$$\begin{aligned} k &= \frac{W}{W + 2s} \\ k' &= \sqrt{1 - k^2} \end{aligned} \tag{10}$$

The contribution to the capacitance from the air ($\epsilon_r = 1$) is given by,

$$C_{\text{air}} = 4\epsilon_0 \frac{K(k)}{K(k')} \tag{11}$$

Therefore the total capacitance per unit length of a CPW is,

$$C_{\text{CPW}} = 2\epsilon_0(\epsilon_r + 1)\frac{K(k)}{K(k')} \tag{12}$$

Under a quasi-static approximation, the effective permittivity due to the dielectric and the air is given by,

$$\begin{aligned} \epsilon_{\text{eff}} &= \frac{C_{\text{CPW}}}{C_{\text{air}}} \\ &= \frac{1 + \epsilon_r}{2} \end{aligned} \tag{13}$$

In addition to this, the phase velocity of the wave is given by,

$$\begin{aligned} v_{\text{ph}} &= \frac{c}{\sqrt{\epsilon_{\text{eff}}}} \\ &= \frac{c}{\sqrt{(1 + \epsilon_r)/2}} \end{aligned} \tag{14}$$

where c is the speed of light in a vacuum. The characteristic impedance if given by,

$$\begin{aligned} Z_0 &= \frac{1}{C_{\text{CPW}} v_{\text{ph}}} \\ &= \frac{30\pi}{\sqrt{\epsilon_{\text{eff}}}} \frac{K(k')}{K(k)} \end{aligned} \tag{15}$$

The result for the case with a finite thickness dielectric substrate is negligibly different as long as the widths of the conductor and gaps are much smaller than the thickness of the dielectric, which will nearly always be the case.

It is also useful to express the phase velocity, $v_{\rm ph}$ and characteristic impedance, Z_0 in terms of inductance and capacitance per unit length, [2]

$$v_{\rm ph} = \frac{1}{\sqrt{L_l C_l}} \tag{16}$$

$$\begin{aligned} Z_0 &= \sqrt{\frac{R_l + j\omega L_l}{G_l + j\omega C_l}} \\ &= \sqrt{\frac{L_l}{C_l}} \qquad\qquad (\text{for } R_l = G_l = 0) \end{aligned} \tag{17}$$

where L_l, C_l, R_l and G_l are the inductance, capacitance, resistance and conductance per unit length respectively, and ω is the angular frequency. Given that we will be working with superconductors justifies the assumption that $R_l = G_l = 0$. In the case above $C_l = C_{\rm CPW}$. It then follows from equations 13, 14 and 16 that the inductance per unit length due to the geometry of the CPW, called the magnetic (or external) inductance is given by, [3]

$$L_l^m = \frac{\mu_0}{4}\frac{K(k')}{K(k)} \tag{18}$$

where μ_0 is the permeability of free space, and k, k' and $K(...)$ are as defined above.

For reasons that I am yet to understand the correct capacitance per unit length of the CPW is actually given by,

$$C_{\rm CPW} = 4\epsilon_0\epsilon_r\frac{K(k)}{K(k')} \tag{19}$$

This should be used in calculations as opposed to the one stated above.

Kinetic inductance

In superconductors, the inductance is determined not only by the temperature independent magnetic inductance, L_l^m but also by the temperature dependent kinetic inductance, $L_l^k(T)$ which originates from the inertia of moving Cooper pairs and can contribute significantly since resistivity is negligible, and therefore charge carrier relaxation times are long. $L_l^k(T)$ is given by, [4]

$$L_l^k(T) = \mu_0\frac{\lambda_L^2(T)}{Wt}\,g(s,W,t) \tag{20}$$

where $\lambda_L(T)$ is the London penetration depth which carries the temperature dependence. $g(s,W,t)$ is a geometric factor defined as,

$$\begin{aligned} g(s,W,t) =& \frac{1}{2k^2K(k)^2}\Bigg(-\ln\left(\frac{t}{4W}\right) \\ &- \frac{W}{W+2s}\ln\left(\frac{t}{4(W+2s)}\right) \\ &+ \frac{2(W+s)}{W+2s}\ln\left(\frac{s}{W+s}\right)\Bigg) \end{aligned} \tag{21}$$

where t is the thickness of the metal layer. The London penetration depth is given by, [5]

$$\lambda_L(T) = \lambda_L(0)\sqrt{\frac{1}{1-(T/T_c)^4}} \tag{22}$$

where T_c is the critical temperature, and the London penetration depth at $T = 0K$ is given by,

$$\lambda_L(0) = 1.05\times10^{-3}\sqrt{\frac{\rho(T_c)}{T_c}} \tag{23}$$

where $\rho(T_c)$ is the normal state resistivity at $T = T_c$. The total inductance per unit length is then the sum of the two contributions,

$$L_l^{tot}(T) = L_l^m + L_l^k(T) \tag{24}$$

Effect of finite thickness metal

The results presented above assumed an infinitely thin metal layer. However in practice this is obviously not the case and a finite thickness can have a small effect. The modifications given in [6] are simple enough that it is worth providing them here. The effective conductor and gap widths are modified as follows,

$$\begin{aligned} W_{\rm eff} &= W + \Delta \\ s_{\rm eff} &= s - \Delta \end{aligned} \tag{25}$$

where,

$$\Delta = \frac{1.25t}{\pi}\left(1 + \ln\left(\frac{4\pi W}{t}\right)\right) \tag{26}$$

where t is the thickness of the metal layer. The affect is however less than 1% if the conductor width is greater than $0.5\mu m$, and is around 0.05% when the conductor width is $10\mu m$.

IV. CPW RESONATORS

A CPW transmission line can be turned into a resonator by terminating it at both ends, either to ground (short) or with an insulating gap (open). If both ends are terminated in the same way then this forms a half-wave

resonator, otherwise it forms a quarter-wave resonator. The frequency, f_n of a resonator is given by,

$$\begin{aligned} f_n &= v_{\text{ph}} \frac{1}{\lambda} \\ &= v_{\text{ph}} \frac{1}{ml} \\ &= \frac{c}{\sqrt{\epsilon_{\text{eff}}}} \frac{1}{ml} \\ &= \frac{1}{\sqrt{L_l C_l}} \frac{1}{ml} \end{aligned} \tag{27}$$

where l is the length of the resonator and m is a factor dependent on the boundary conditions, i.e. $m = \frac{4}{2n^*}$ for half-wave and $m = \frac{4}{(2n^*-1)}$ for quarter-wave resonators, where n^* is the harmonic mode.

Temperature dependence of resonance frequency

The only temperature dependent parameter of the resonance frequency (equation 27) is from the total inductance per unit length, L_l which in turn originates from the kinetic inductance per unit length, L_l^k (equation 20), which in turn originates from the London penetration depth, $\lambda_L(T)$ (equation 22). Experimental data of the normalised resonance frequency against temperature is shown in Figure 4 for 11 different over and under-coupled resonances and resonance frequencies.

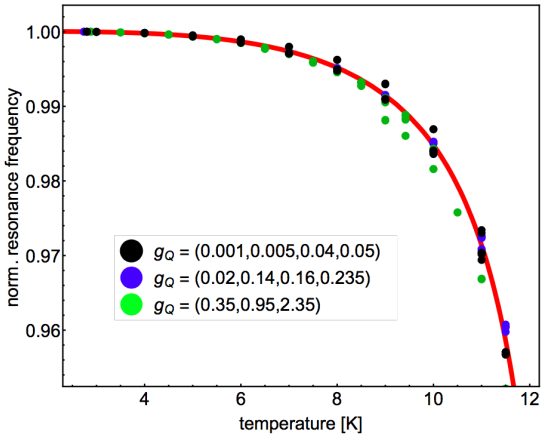

FIG. 4. Normalised resonance frequency shift as a function of temperature for 3 different samples and 11 different over and under-coupled resonances and resonance frequencies ranging from 5 GHz to 30 GHz using half-wave resonators. The red line is a fit using $f_n(T)/f_n(3) = \sqrt{L_l(3)/L_l(T)}$ (derived from equations 18, 20, 24 and 27), and using measured data for $T = 3K$. [5]

Coupled CPW resonators

A CPW resonator is not of much use unless it is coupled in some way to controllable experimental apparatus. For a half-wave resonator this is generally achieved by constructing the resonator out of what is already a connected transmission line, simply by adding two insulating gaps as illustrated in Figure 5. A quarter-wave resonator is generally coupled to a separate electrically continuous transmission line, called a *feedline* as illustrated in Figure 6. The coupling capacitance is then determined by the length of the coupling section (Figure 6c, called an *elbow connector*) and its separation from the feedline. It is not generally trivial to compute this capacitance and we refer to this challenge later when discussing the parameters of the design and simulations.

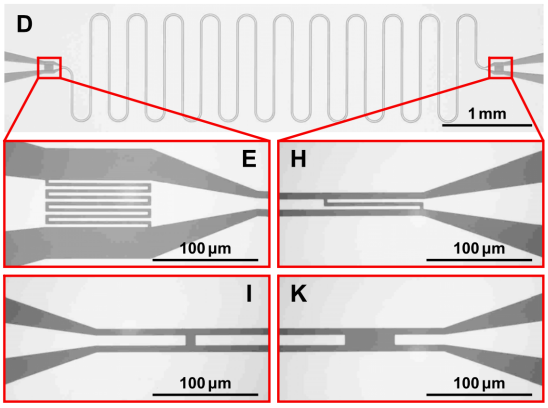

FIG. 5. Example of a half-wave resonator, constructed as two insulating gaps added to a CPW transmission line. The gaps can be simple as shown in sub-figures I and K, or one can increase the coupling capacitance by using an interdigitated design such as those shown in sub-figures E and H. [2]

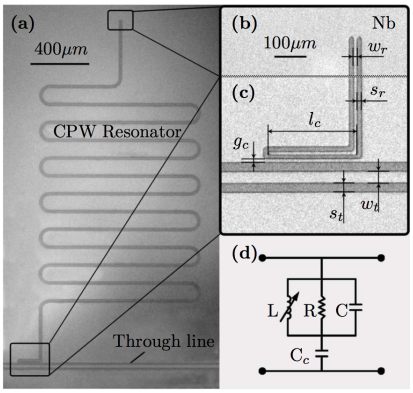

FIG. 6. Example of a quarter-wave resonator, constructed as a transmission line with an open termination at the coupling end and a shorted termination at the other. The separate uninterrupted transmission line (feedline) is used to couple the quarter-wave resonator to the experimental apparatus. [7]

Coupling a resonator to the outside world has a number of affects as compared to the isolated resonator, including modifying the quality factor, Q and the resonance

frequency, f_n. The latter is given by, [2]

$$f_n^* = \frac{1}{m\sqrt{L(C+C^*)}} \tag{28}$$

where $L = L_l\, l$, $C = C_l\, l$, m is as before and C^* is the contribution of the capacitance due to coupling given by,

$$C^* = \frac{C_\kappa}{1 + (f_n C_\kappa R_L \pi)^2} \tag{29}$$

where C_κ is the coupling capacitance, f_n if the uncoupled resonance frequency and R_L is the load resistance, usually 50Ω. To obtain a rough feeling for the magnitude of such shifts in resonance frequency, f_n, data from [2] is shown in Figure 7. The shifts are up to around 65MHz in this case.

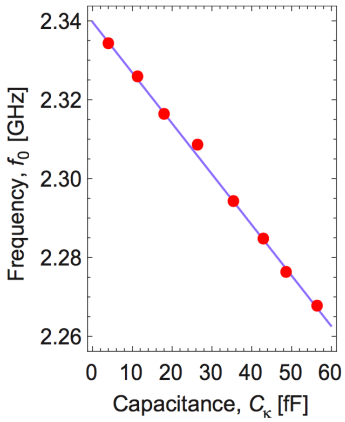

FIG. 7. Data from [2] showing the shifts in the fundamental resonance frequency, f_0 as a function of coupling capacitance, C_κ. The shifts are up to around 65 MHz.

The quality factor of a resonator, Q is a measure of the width of a resonance, $Q = \frac{f_n}{\Delta f_n}$. An isolated resonator has an internal quality factor, Q_{int} which is generally dependent on material quality and fabrication. The internal quality factor is given by, [2, 8]

$$Q_{\text{int}} = \frac{1}{m}\frac{\pi}{\alpha l} \tag{30}$$

where m is as before, α is the amplitude attenuation per unit length and l is the length. When coupled to the outside world there is also a contribution referred to as the coupling (or external) quality factor, Q_{ext}. The external quality factor is given by, [8, 9]

$$Q_{\text{ext}} = \frac{\pi}{m q_{\text{in}}^2} \tag{31}$$

where q_{in} is given by,

$$\begin{aligned} q_{\text{in}} &= \omega_n C_\kappa Z_0 \\ &= 2\pi f_n C_\kappa Z_0 \end{aligned} \tag{32}$$

The total, or loaded quality factor is given by, [2]

$$\frac{1}{Q_L} = \frac{1}{Q_{\text{int}}} + \frac{1}{Q_{\text{ext}}} \tag{33}$$

The ratio of the two, called the Q-coupling ratio,

$$g_Q = \frac{Q_{\text{int}}}{Q_{\text{ext}}} \tag{34}$$

determines whether the resonance width, Δf_n is limited by internal ($g_Q \ll 1$) or external losses ($g_Q \gg 1$). These regimes are referred to as *under-coupled* and *over-coupled* respectively. The boundary between these, where $g_Q = 1$ is called critical coupling. Data in Figure 9 shows the loaded quality factor, Q_L for multiple half-wave resonators with varying coupling capacitances. Notice that the highest quality factors are achieved in the under-coupled regime where the coupling capacitance, C_κ is low, but does not improve with decreasing C_κ.

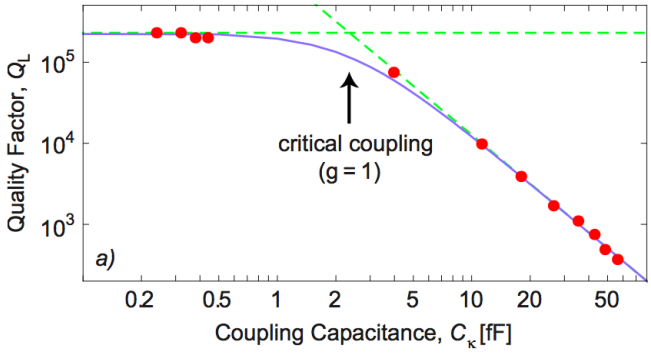

FIG. 8. Data from multiple half-wave resonators with different coupling capacitances showing the affect on the loaded quality factor, Q_L. At low coupling capacitance ($C_\kappa < 1$ fF), where $g_Q < 1$ we are in the under-coupled regime. Here we are limited by internal losses which are independent of coupling capacitance. At high coupling capacitance ($C_\kappa > 5$ fF), where $g_Q > 1$ we are in the over-coupled regime. Here we are limited by external losses which scale exponentially with coupling capacitance. Where $g_Q = 1$ is called the critical coupling. [2]

The insertion loss, L_0 of a resonator describes the deviation of peak transmission from unit, and is given by,

$$L_0 = -20 \log\left(\frac{g}{g+1}\right) \text{dB} \tag{35}$$

where g is the Q-coupling ratio. The dependence of the insertion loss on coupling capacitance is illustrated in Figure [REF].

Using higher harmonics

Sometimes one might want to use a higher harmonic of a resonator ($n^* > 1$) in order to achieve higher resonance frequencies, f_n without reducing the length of the resonator. An example of this could be if one wanted to couple atoms flying over the resonator. The required frequencies to match an atomic transition may be quite high but one wouldn't want to reduce the length of the resonator too much because this would reduce the time the atoms had to interact, hence one could just use a

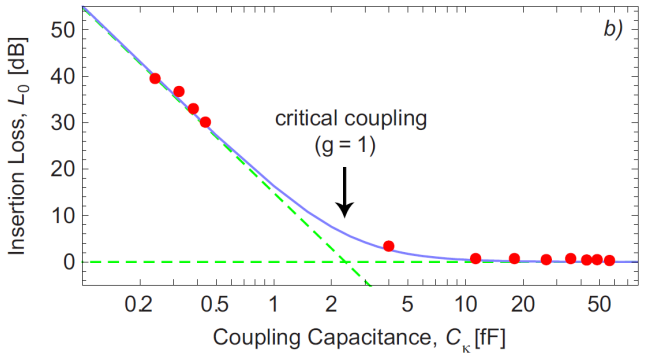

FIG. 9. Data from multiple half-wave resonators with different coupling capacitances showing the affect on the insertion loss, L_0. At low coupling capacitance ($C_\kappa < 1$ fF), where $g_Q < 1$ we are in the under-coupled regime. Here we are limited by internal losses which are independent of coupling capacitance. At high coupling capacitance ($C_\kappa > 5$ fF), where $g_Q > 1$ we are in the over-coupled regime. Here we are limited by external losses which scale exponentially with coupling capacitance. Where $g_Q = 1$ is called the critical coupling. [2]

higher harmonic. There are however trade off's to be considered. For one the quality factor, Q_L reduces with increasing n^*. A measurement of this is shown Figure 10.

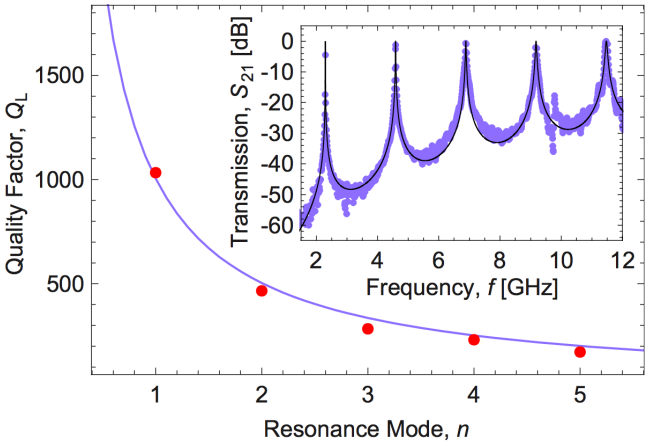

FIG. 10. The loaded quality factor, Q_L for a resonator decreases with increasing harmonic, n^*. Although it is sometimes beneficial to use a higher harmonic to achieve higher frequencies, f_n, the reduction in the quality factor needs to be considered. [2]

Other sources of loss

Besides the sources of loss associated with the quality of the superconducting material, other sources of loss include radiative, resistive and dielectric losses. Radiative losses are small in CPW resonators [10]. Resistive losses are negligible far below T_c and at frequencies well below the superconducting gap [11]. Dielectric losses however are likely to limit the internal quality factor, Q_{int} as discussed in [12, 13]

ABCD Transmission matrix

The ABCD matrix can be used to fit the transmission/reflection resonance peaks of a resonator. The matrix is defined as,

$$\begin{bmatrix} A & B \\ C & D \end{bmatrix} = \begin{bmatrix} 1 & Z_{in} \\ 0 & 0 \end{bmatrix} \begin{bmatrix} t_{11} & t_{12} \\ t_{21} & t_{22} \end{bmatrix} \begin{bmatrix} 1 & Z_{out} \\ 0 & 0 \end{bmatrix} \tag{36}$$

where,

$$t_{11} = t_{22} = \cosh \gamma l \tag{37}$$

$$t_{12} = Z_0 \sinh(\gamma l) \tag{38}$$

$$t_{21} = \frac{1}{Z_0} \sinh(\gamma l) \tag{39}$$

where Z_0 is the characteristic impedance, and $\gamma = \alpha + i\beta$ where α is the amplitude attenuation coefficient and β is given by,

$$\beta = \frac{\omega_n}{v_{ph}} = \omega_n \sqrt{L_l C_l} = \omega_n \frac{\sqrt{\epsilon_0}}{c} \tag{40}$$

The transmission parameter, S_{21} is then given by,

$$S_{21} = \frac{2}{A + \frac{B}{R_L} + CR_L + D} \tag{41}$$

where R_L is the load resistance.

V. RESONATOR DESIGN

The purpose of discussing the properties of CPW resonators above has been in order to design a resonator for use in hybrid atomic-cQED (circuit quantum electrodynamics) experiments involving the interaction between helium atoms in circular Rydberg states and superconducting resonators, as proposed in [14]. In this section we; discuss the design criteria of such a resonator, present a proposed design for meeting these criteria, as well as results of simulations for this design which were used to determine the coupling parameters, and finally we consider the design of a mount for the sample.

Design criteria

The design criteria for the resonator are as follows,

1. **50Ω line impedance**: For both the resonator and feedline in order to match the impedance of the connected electronics and hence minimise reflections.

2. **Resonance frequency, f_n in the range of Rydberg transitions with 60< n <80**: This is roughly the range of n that will be used in the experiments. The lower bound for n is set by the requirement that the length of the resonators be of the order of mm. The upper bound is loosely set by a decreasing ionisation energy and increasing sensitivity.
3. **High loaded quality factor, Q_L**: Such that coherence times of the resonator are long enough to observe multiple Rabi oscillations in the atoms.
4. **Straight region longer than 5mm for the Rydberg atoms to fly over and interact with**: The interaction time should be long enough to observe several Rabi oscillations. The velocity of the supersonic atom beam will be around $1720ms^{-1}$ [15], so a length of 5mm leads to an interaction time of $2.91\mu s$, which with a interaction strength of $g \approx 10$MHz should be enough to observe about 25 Rabi oscillations [14].
   (a) **This region should be at least 2mm from other sources of microwaves**: Such as the feedline in order to minimise unintended interactions.
   (b) **The electric field in this interaction region should preferably contain a maximum**: In order to maximise the interaction strength.
5. **Shorted to ground**: Charged particles adsorbed on/near the resonator would cause it to accumulate charge. This would be avoided by shorting the resonator to ground.
6. **Controllable capacitive coupling to the feedline**: In order to control the Q-coupling ratio g_Q and hence whether the resonator is in the over or under-coupled regime.
7. **Accessible connection to the feedline**: Such that the feedline can be connected to an external microwave source. The conductor of the feedline as is will likely too small to wire bond to.

Proposed design

The proposed design, illustrated in Figure 11 addresses each of the design requirements as follows,

1. **50Ω line impedance**: The characteristic impedance is given by equation 15. Using a 2:1 conductor:gap width ratio will lead to an impedance close to 50Ω. Values of $20{:}10\mu m$ should be reasonable to fabricate and provide a strong enough interaction with the atoms whilst having a wide enough field distribution to interact with the whole atom beam cross-section in a roughly uniform way.
2. **Resonance frequency, f_n in the range of Rydberg transitions with 60< n <80**: Within these bounds, the required length of the resonator ranges from 0.993mm (Rydberg state $n = 60$, 1^{st} harmonic ($n^* = 1$) of a quarter-wave resonator) to 18.711mm (Rydberg state $n = 80$, 4^{th} harmonic ($n^* = 4$) of a half-wave resonator). These are well within the fabrication capabilities available.
3. **High loaded quality factor, Q_L**: Although reasonable Q resonators can been achieved with normal-state metals, the highest Q values are achieved using superconducting materials. The experiment will be cryogenically cooled using a pulse tube down to around 3-4K. Therefore a superconductor with a critical temperature, T_c greater than this is required. Pure Niobium, Nb has a T_c of 9.2K [16] making it an option. Niobium Nitride, NbN will also go superconducting, but with a T_c around 16.2K depending on the concentration of Nitrogen [17]. This will be discussed in more detail in section VI.
4. **Straight region longer than 5mm for the Rydberg atoms to fly over and interact with**: This condition places a lower bound on the combination of the Rydberg state, n and the resonator harmonic, n^* used. For example, at $n = 60$ the harmonics that match this criteria are $n^* \geq 4$ for a quarter-wave resonator and $n^* \geq 3$ for a half-wave resonator. This however leaves little excess length for separating the resonator from the feedline, leading to our next requirement.
   (a) **This region should be at least 2mm from other sources of microwaves**: This leads to a minimum required length of 7.2mm (including 0.2mm for the curved sections and the coupler). For $n = 70$, the matching harmonics are now $n^* \geq 3$ for both the quarter and half-wave resonators. Note that the quality factor, Q decreases with n^* as shown in Figure 10. The trade off is then between high Q and low n. $n = 70$, $n^* = 3$ is a good compromise.
   (b) **The electric field in this interaction region should preferably contain a maximum**: For a quarter-wave resonator coupled to a feedline, the single electric field maximum is at the coupler. The other end, which is shorted to ground (see Figure 11c) has an electric field minimum. Therefore in the 1^{st} harmonic, $n^* = 1$ no maximum is present in the interaction region. This is not the case for $n^* > 1$. Half-wave resonators should not have this issue.
5. **Shorted to ground**: This can be achieved by using a quarter-wave resonator which inherently has one end shorted to ground (see Figure 11c). This is the main advantage over half-wave resonators which led to the decision to use a quarter-wave resonator. It is possible to short a half-wave resonator using thin strips, however this would greatly complicate the fabrication process.
6. **Controllable capacitive coupling to the feedline**: By using a so-called *elbow coupler* (see Figure 11b) whose length and separation from the feedline can be varied, one can control the capacitive cou-

pling.

7. **Accessible connection to the feedline**: By increasing the widths of the feedline whilst maintaining the 2:1 conductor:gap ratio, the line impedance will stay the same but the centre conductor will be large enough to wire bond to. Values of 300:150μm should be reasonable. Care should be taken that the gap width is much smaller than the substrate thickness, especially if the back of the substrate is coated with a conductor. This is because the dominant source of capacitance for the center conductor should be from the top layer ground plane.

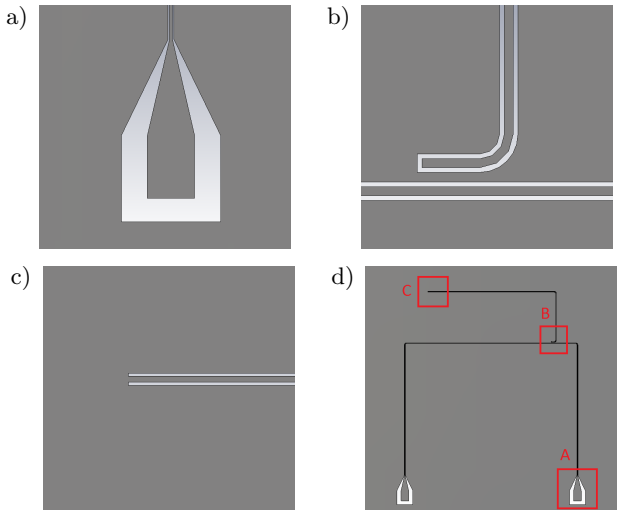

FIG. 11. **d)** Proposed design for the quarter-wave resonator and feedline. The longest straight section of the resonator will be where the atoms fly over, therefore its length is to be maximised. Interaction with the feedline should be minimised, therefore some length is sacrificed in order to increase the separation. **b)** The length of the elbow connector and it's separation from the feedline can be varied to control the coupling capacitance, C_κ. **c)** An advantage of the quarter-wave over the half-wave resonator is that the end is shorted to ground. This has the affect of dissipating any charge which builds up on the resonator as atoms adsorb onto the surface. **a)** The feedline is terminated with pad connectors which preserve the conductor:gap ratio as to maintain an impedance of around 50Ω, but to increase the surface area available for wire bonding the feedline to an external microwave source.

Simulations

Computer simulations can be used to predict (at least approximately) some of the properties of our proposed resonator design. For this we use the very creatively named CST (Computer Simulation Technology) Microwave Suite®. CST in fact uses finite integration in technique (FIT) instead of the (arguably) more well known finite element method (FEM) used by software packages such as HFSS (High Frequency Structural Simulator). For our current practical purposes the difference is irrelevant, both would give similar results.

The purpose of running these simulations is not an attempt to predict the exact results expected from the real device, but rather to aid in the design process by; having a decent model that may help identify flaws in the design, visualise the electric field distribution, and determine parameters such as the coupler length and separation from the feedline. The latter is actually difficult to determine. We saw in Figure 9 that depending on the coupling capacitance the resonator is in the over or under-coupled regimes and hence the loaded quality factor, Q_L is limited by either external or internal factors respectively. In order achieve high loaded quality factors it is therefore important to choose coupling parameters carefully in order to find oneself in the under-coupled regime.

Coupling parameters

To this end we performed some simulation experiments in which we varied the length of the coupler and its separation from the feedline and monitored the quality factor. The model used is illustrated in Figure 12, where the metal layer has been reduced to only the regions of importance in order to minimise RAM usage and run time. The results of these experiments are shown in Figure 13. Note that both axis are inverted relative to Figure 9 because a small peak-to-trough frequency relates to a high quality factor, and a small coupler-feedline separation relates to a high capacitance. By comparing these to Figure 9, it seems as though the resonator is always in the over-coupled regime, it is not becoming limited by internal factors. This may make sense given that the metal layer was modelled as a PEC (perfect electrical conductor), and therefore shouldn't be limited by internal factors.

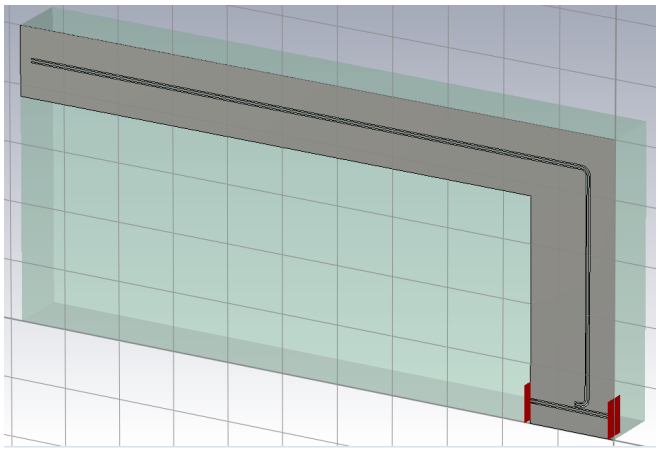

FIG. 12. Model used for the CST simulations of the proposed resonator design. The model was reduced to just the resonator and a small section of the feedline in order to reduce the number of required mesh elements and hence the RAM requirements and run time. The metal layer (light grey) is modelled as a PEC (perfect electrical conductor). The substrate (opaque green) is modelled as loss-free silicon. The two red regions represent the microwave ports.

This is the only method found so far that can pro-

vide an insight into determining the coupling parameters. Perhaps it will be much more instructive to simply fabricate resonators with different coupling parameters, determine their quality factors and hence the over and under-coupled regimes.

Mount

Designing and fabricating the sample itself is not enough to connect it to the rest of the experiment. A custom mount will be required to interface between the samples feedline and the external microwave source. An example of such a mount used for a similar experiment using a half-wave resonator is shown in Figure 14. A similar concept tailored for a quarter-wave resonator should be ideal. The main difference being that both input and output ports will have to be connected to the same mount block such as not to cross the line of the atom beam.

VI. RESONATORS MATERIALS

We use this section as an opportunity to discuss some of the considerations that were taken into account when choosing materials. The two main ones being the superconducting material used for the metal layer and the substrate material on which the metal layer is placed.

Superconducting material

We've mentioned that the experiment will be cryogenically cooled using a pulse tube down to 3-4K. This means that materials such as Aluminium with a $T_c = 1.2$K would no be suitable. Instead we will use some form of Niobium (Nb), which when pure has a $T_c = 9.2K$ [16] and when mixed with Nitrogen to form Niobium Nitride (NbN) has a $T_c = 16.2$K [17]. Some groups have also used Niobium Titanium Nitride (NbTiN) [5], however this have remained a niche material and the capability is not available at the LCN. It is not clear what the advantages are anyway, so we restrict our discussion to Nb and NbN. We summarise the pro's and con's of each below.

Niobium (Nb):

Pro's:

- **Lower kinetic inductance,** L^k: Leading to more predictable resonance frequencies, f_n because the amount of Nitrogen in the sputtering chamber will determine the amount of L^k and hence the resonance frequency shift.
- **Simpler fabrication process**: No need to include Nitrogen in the sputter chamber. This also improves reproducibility.

Con's:

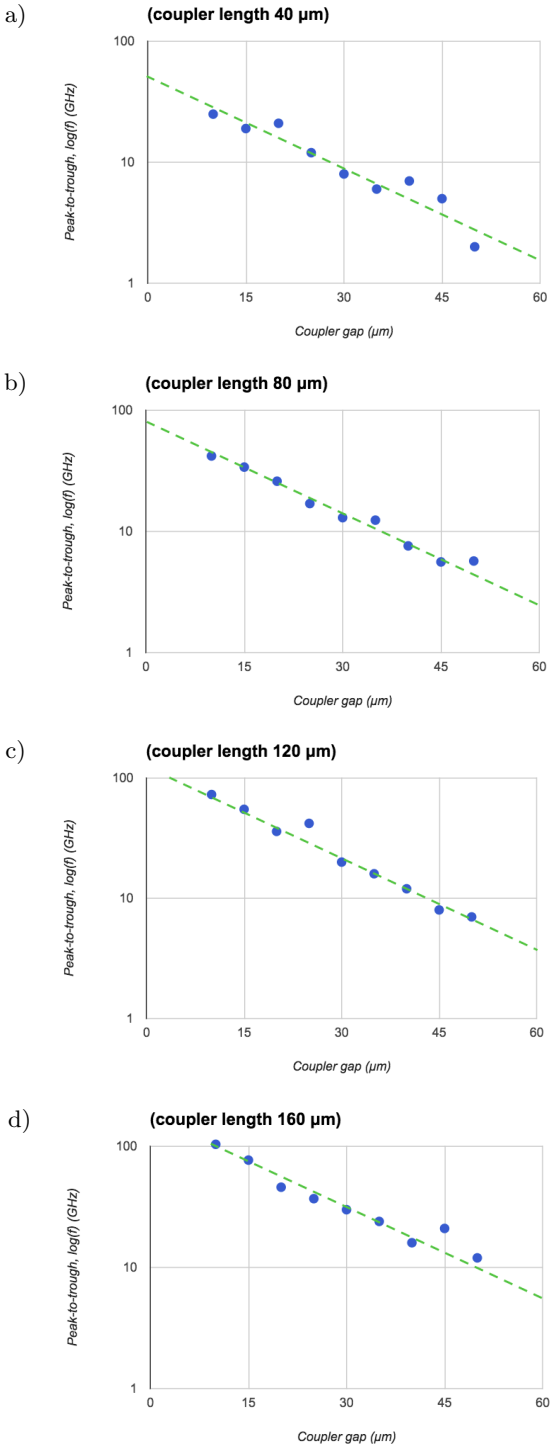

FIG. 13. Simulations of quality factor for various coupling parameters. The reflection resonance peak, $S_{1,2}$ in the simulations had the shape of a dispersive Lorentzian. We therefore use as a measure of quality factor the frequency difference between the peak and trough of the resonance. Three different coupler lengths were used, **a)** $40\mu m$ **b)** $80\mu m$ **c)** $120\mu m$ **d)** $160\mu m$. For each the coupler separation from the feedline was varied from $10\mu m$ to $50\mu m$ in steps of $5\mu m$. The dotted lines are a fit to the data illustrating an exponential relationship similar to that of the over-coupled regime in Figure 9.

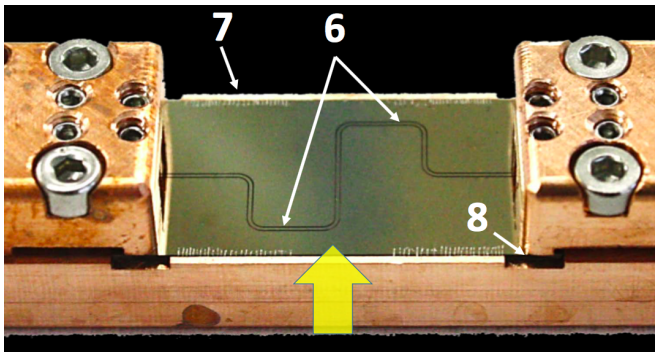

FIG. 14. Example of a half-wave resonator mount used in [5]. **6)** Insulating gaps in a CPW transmission line to form a half-wave resonator. **7)** Wire bonds between the ground plane of the sample and ground plane of the mount. Notice that these are absent in the vicinity of the atom beam, indicated by the yellow arrow. **8)** The ground plane of the sample is insulated from the blocks of the mount.

- **Sensitive to contamination**: Any contamination from the sputtering process will have detrimental and unpredictable affects on the internal quality factor, Q_{int} and resonance frequency, f_n. The sputtering chambers in the LCN cleanroom are multi material which means that some amount of cross contamination is likely and variable between runs.
- **Susceptible to oxidisation**: Pure Niobium will oxidise slowly which will have detrimental affects on the internal quality factor, Q_{int}.

Niobium Nitride (NbN):

Pro's:

- **Less sensitive to contamination**: NbN is already considered a *dirty* superconductor because of the Nitrogen, therefore extra contaminants will have little affect.
- **Less prone to oxidisation**: NbN oxidises much slower than Nb, therefore doesn't suffer from the reduction in internal quality factor, Q_{int}.
- **Higher T_c**: Although there is more kinetic inductance L^k, the T_c is higher which means that at $T = 3 - 4$K, $\frac{T}{T_c}$ is lower and the affect of L^k is not as much as one might expect.
- **Well characterised process**: The NbN process has been well characterised at the LCN by John Burnett and is used widely by several groups including John Morton's and Paul Warburton's groups.

Con's:

- **Slightly more complicated fabrication process**: The additional complexity in knowing a recipe for the amount of Nitrogen in the sputtering chamber is needed, although this is well characterised.
- **Higher kinetic inductance, L^k**: NbN is a dirty superconductor and therefore has a higher L^k which will increase the downwards shift in resonance frequency. This is fine if accounted for, but just adds an extra consideration.

For these reasons it is recommended that NbN is used, at least for the first devices.

Substrate material

The internal quality factor, Q_{int} of the resonator will depend strongly on the substrate used as this will quickly become the limiting factor if care isn't taken. In this subsection we discuss the considerations in choosing a substrate.

TO DO. (Need to find out more about this first.)

VII. FABRICATION

In this section we discuss different aspects of the fabrication of the resonator, from designing and buying the photo mask, to the steps involved in the cleanroom.

Photo mask

The proposed mask design is shown in Figure 15, designed using KLayout and CleWin.

Process

In this section we give an outline of the steps involving in fabricating our proposed resonator.

Dicing:
Cleaning:
Sputtering:
Photo lithography (PL): .

Spin coating:
UV exposure:
Developing:

Electron beam lithography (EBL):
Etching:
Wire bonding:

Costs

In this section we outline the costs of the fabrication process.

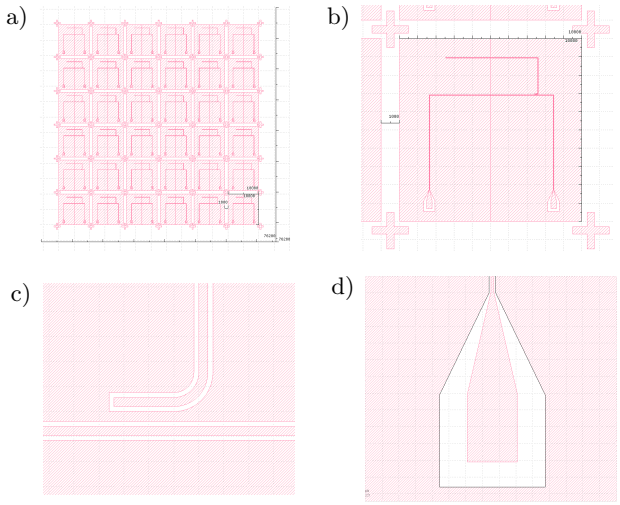

FIG. 15. **a)** Full design for the photo mask consisting of 6x6 tiles, each measuring 10×10mm with inter-tile spacing of 1mm. The mask is designed for a 4 inch mask, which after allowing for a $\frac{1}{2}$ inch border leaves 7.62×7.62mm area for the design. Alignment marks are placed around each tile corner to aid with mask alignment. **b)** Single 10×10mm tile consisting of a quarter-wave resonator coupled to a feedline which itself is terminated by end connectors. **c)** Elbow coupler. **d)** End connector.

VIII. EXPERIMENTS

Extracting resonator parameters

[1] R. N. Simons. *Coplanar Waveguide Circuits, Components, and Systems*. John Wiley & Sons (2001).

[2] M. Göppl, A. Fragner, M. Baur *et al.* Coplanar waveguide resonators for circuit quantum electrodynamics. *Journal of Applied Physics*, **104** (2008).

[3] W. Rauch, E. Gornik, G. Sölkner *et al.* Microwave properties of YBa2Cu3O7x thin films studied with coplanar transmission line resonators. *Journal of Applied Physics*, **73**, 1866 (1993).

[4] K. Watanabe, K. Yoshida, T. Aoki *et al.* Kinetic Inductance of Superconducting Coplanar Waveguides. *Japanese Journal of Applied Physics*, **33**, 5708 (1994).

[5] T. S. Thiele. *Coherent manipulation of Rydberg atoms close to surfaces at cryogenic temperatures*. Ph.D. thesis, ETH Zurich (2016).

[6] K. C. Gupta, R. Garg, I. J. Bahl *et al. Microstrip Lines and Slotlines*. Artech House, Inc. (1996).

[7] H. Li, Y. Wang, L. Wei *et al.* Experimental demonstrations of high-Q superconducting coplanar waveguide resonators. *Chinese Science Bulletin*, **58**, 2413 (2013).

[8] A. P. Sears. *Extending Coherence in Superconducting Qubits: from microseconds to milliseconds*. Ph.D. thesis, Yale University (2013).

[9] D. I. Schuster. *Circuit Quantum Electrodynamics*. Ph.D. thesis, Yale University (2007).

[10] J. Browne. Broadband amps sport coplanar waveguide. *Microwaves*, **26**, 131 (1987).

[11] L. Frunzio, A. Wallraff, D. Schuster *et al.* Fabrication and characterization of superconducting circuit QED devices for quantum computation. *IEEE Transactions on Applied Superconductivity*, **15**, 860 (2005).

[12] A. D. O'Connell, M. Ansmann, R. C. Bialczak *et al.* Microwave dielectric loss at single photon energies and millikelvin temperatures. *Applied Physics Letters* (2008).

[13] J. M. Martinis, K. B. Cooper, R. McDermott *et al.* Decoherence in Josephson qubits from dielectric Loss. *Physical Review Letters* (2005).

[14] A. Morgan and S. Hogan. Coupling atoms in circular Rydberg states to chip-based microwave resonators. *PhD Proposal* (2016).

[15] S. D. Hogan, J. A. Agner, F. Merkt *et al.* Driving Rydberg-Rydberg transitions from a coplanar Microwave Waveguide. *Phys. Rev. Lett.*, **108**, 063004 (2012).

[16] M. Peiniger and H. Piel. A Superconducting Nb3Sn Coated Multicell Accelerating Cavity. *IEEE Transactions on Nuclear Science*, **32**, 3610 (1985).

[17] E. A. Antonova, D. R. Dzhuraev, G. P. Motulevich *et al.* Superconducting energy gap of niobium nitride. *Sov. Phys. - JETP*, **53** (1981).